NIH Public Access
Author Manuscript
NMR Biomed. Author manuscript; available in PMC 2015 November 01.

Published in final edited form as:
NMR Biomed. 2014 November ; 27(11): 1419–1426. doi:10.1002/nbm.3221.

MOLLI and AIR T1 Mapping Pulse Sequences Yield Different Myocardial T1 and ECV Measurements

KyungPyo Hong[1,2] and **Daniel Kim**[2]

[1]Department of Bioengineering, University of Utah, Salt Lake City, UT, 84112

[2]UCAIR, Department of Radiology, University of Utah, Salt Lake City, UT, 84108

Abstract

Both post-contrast myocardial T1 and extracellular volume (ECV) have been reported to be associated with diffuse interstitial fibrosis. Recently, the cardiovascular magnetic resonance (CMR) field is recognizing that post-contrast myocardial T1 is sensitive to several confounders and migrating towards ECV as a measure of collagen volume fraction. Several recent studies using widely available Modified Look-Locker Inversion-recovery (MOLLI) have reported ECV cutoff values to distinguish between normal and diseased myocardium. It is unclear if these cutoff values are translatable to different T1 mapping pulse sequences such as arrhythmia-insensitive-rapid (AIR) cardiac T1 mapping, which was recently developed to rapidly image patients with cardiac rhythm disorders. We sought to evaluate, in well-controlled canine and pig experiments, the relative accuracy and precision, as well as intra- and inter-observer variability in data analysis, of ECV measured with AIR as compared with MOLLI.

In 16 dogs, as expected, mean T1 was significantly different ($p < 0.001$) between MOLLI (891±373 ms) and AIR (1071±503 ms), but, surprisingly, mean ECV between MOLLI (21.8±2.1%) and AIR (19.6±2.4%) was also significantly different ($p < 0.001$). Both intra- and inter-observer agreements in T1 calculations were higher for MOLLI than AIR, but intra- and inter-observer agreements in ECV calculations were similar between MOLLI and AIR. In 6 pigs, coefficient of repeatability (CR), as defined by Bland-Altman analysis, of T1 was considerably lower for MOLLI (32.5 ms) than AIR (82.3 ms), and CR of ECV was also lower for MOLLI (1.8%) than AIR (4.5%).

In conclusion, this study shows that MOLLI and AIR yield significantly different T1 and ECV values in large animals and that MOLLI yields higher precision than AIR. Findings from this study suggest that CMR researchers must consider the specific pulse sequence when translating published ECV cutoff values into their own studies.

Keywords

Diffuse myocardial fibrosis; post-contrast myocardial T_1; extracellular volume fraction; CMR; T1 mapping

Please send correspondence to: Daniel Kim, The University of Utah, 729 Arapeen Drive, Salt Lake City, Utah 84108, Phone: (801) 587-3861, Fax: (801) 585-3592, daniel.kim@hsc.utah.edu.

NIH-PA Author Manuscript
NIH-PA Author Manuscript
NIH-PA Author Manuscript

NIH-PA Author Manuscript

NIH-PA Author Manuscript

NIH-PA Author Manuscript

Introduction

Diffuse myocardial fibrosis is a marker of adverse structural remodeling in a variety of heart diseases. While myocardial biopsy is the current gold standard for assessment of diffuse cardiac fibrosis, it is rarely clinically indicated due to its associated non-negligible risk of complications and sensitivity to sampling errors. Cardiovascular magnetic resonance (CMR) is the only proven non-invasive modality for quantifying diffuse myocardial fibrosis. Both post-contrast myocardial T1 (1–4) and myocardial extracellular volume (ECV) fraction (4–8), derived from native and post-contrast myocardial and blood T1 measurements, have been associated with diffuse interstitial fibrosis burden. These promising developments and findings are establishing the foundation towards non-invasive myocardial biopsy with CMR (9).

Among several different cardiac T1 mapping pulse sequences reported in literature (10–19), modified Look-Locker Inversion-recovery (MOLLI)(10) is the most widely used and commercially available as a work-in-progress. While MOLLI has been an important development in CMR, it requires a long scan time (17 heart beats) and is known to be sensitive to rapid heart rate and arrhythmia (20,21), T2 and magnetization transfer effects (19), and inversion pulse efficiency (22,23). These limitations are particularly concerning for imaging patients with irregular heart rhythm and/or rapid rates (e.g., atrial fibrillation). In response, we developed an arrhythmia-insensitive-rapid (AIR) cardiac T1 mapping pulse sequence (15) based on transmit radio-frequency field (B_1+)-insensitive saturation-recovery of magnetization preparation (24), in order to enable accurate cardiac T1 mapping in patients with rapid heart rate and/or arrhythmia. Because AIR cardiac T1 mapping is relatively new, reports of its performance are limited to a few preliminary studies (15,25–27).

Recently, the CMR field is recognizing that post-contrast myocardial T1 is sensitive to confounders such as renal function, hematocrit, magnetic field strength, contrast agent type and dosage, and specific delayed imaging time after administration of contrast agent. Hence, the CMR field is migrating towards ECV, because it is largely insensitive to such confounders. Several recent studies using MOLLI have reported ECV cutoff values to distinguish between normal and diseased myocardium (4,28–30). It is unclear if these cutoff values are translatable to different T1 mapping pulse sequences such as AIR and others. This is especially important since other studies have reported that inversion-recovery based T1 mapping pulse sequences produce lower accuracy but higher precision than saturation-recovery based T1 mapping pulse sequences (31). As an important step towards clinical and pre-clinical utility of AIR, it is necessary to determine whether AIR and MOLLI yield comparable myocardial ECV (i.e., determine if ECV cutoff values established by MOLLI are translatable to AIR). The purpose of this study was to evaluate, in well-controlled canine and pig experiments, the relative accuracy and precision, as well as intra- and inter-observer variability in data analysis, of ECV measured with AIR as compared with MOLLI.

NIH-PA Author Manuscript

NIH-PA Author Manuscript

NIH-PA Author Manuscript

Experimental

MRI Hardware

CMR was performed on two 3T whole-body MRI scanners (Verio and Tim Trio, Siemens Healthcare, Erlangen, Germany), each equipped with a gradient system capable of achieving a maximum gradient strength of 45 mT/m and a slew rate of 200 T/m/s. The radio-frequency excitation was performed using the body coil. The pig experiments were performed on the Tim Trio MRI scanner with standard receiver coil arrays (typically 12-elements total). Canine experiments were performed on the Verio MRI scanner with a 32-element cardiac coil array (RAPID MR International, Columbus, OH).

Pulse Sequence

We used the MOLLI (Siemens WIP # 448) and AIR cardiac T1 mapping pulse sequences with balanced steady-state of free precession (b-SSFP) readout and the following identical set of imaging parameters: field of view = 280 mm × 210 mm (phase-encoding), image acquisition matrix = 192 × 144 (phase-encoding), spatial resolution = 1.5 mm × 1.5 mm, slice thickness = 8 mm, generalized autocalibrating partially parallel acquisitions (GRAPPA)(32) acceleration factor 1.8, TR = 2.7 ms, TE = 1.1 ms, flip angle = 35°, receiver bandwidth = 930 Hz/pixel, saturation-recovery time delay (TD) = 600 ms, and temporal resolution = 217 ms.

Figure 1 shows pulse sequence diagrams of AIR and MOLLI. Briefly, AIR acquires one proton-density weighted image and one T1 weighted image with breath-hold duration = 2–3 heart beats (depending on heart rate). MOLLI acquires 11 T1 weighted images following three inversion pulse modules (3-3-5, as shown). In this study, for AIR, we used "paired" consecutive phase-encoding steps in centric k-space ordering to minimize b-SSFP artifacts arising from eddy currents (33). For MOLLI with breath-hold duration = 17 heart beats, we used the inversion times (i.e., 3-3-5) and flip angle of 35 as previously described (34).

Animal Subjects

Animal MRI was performed in accordance with protocols approved by our Institutional Animal Care and Use Committee. We note that this CMR study was added onto separate canine and pig CMR experiments, and that cardiac tissues were not made available for histolic analysis. We note that pig experiments were conducted after the canine experiments were completed, in order to acquire additional data for analysis of precision (i.e., since repeated measurements were not made in canines). For both canine and pig experiments, animals were anesthetized with propofol (5–8 mg/kg, IV) for intubation and subsequently ventilated and maintained in a surgical plane of anesthesia with 1.5–3% isoflurane. Ventilation was controlled using a ventilator (DRE Premier XP MRI-Compatible Veterinary Anesthesia Machine, DRE Veterinary, Louisville, KY). Breath-hold CMR image acquisitions were performed at end-expiration with the respirator suspended. Heart rate, core body temperature, blood pressure, end-tidal CO_2, and oxygen saturation were continuously monitored and maintained within normal ranges. Blood was drawn during the CMR exam for hematocrit calculation.

NIH-PA Author Manuscript

NIH-PA Author Manuscript

NIH-PA Author Manuscript

Experiment 1: Evaluation of Relative Accuracy in Canines

We imaged 16 mongrel dogs with normal myocardium (8 males and 8 females; 29.9 ± 4.2 kg) to assess the agreement of myocardial T1 and ECV measurements between MOLLI and AIR. In each dog, we performed native cardiac T1 mapping and post-contrast cardiac T1 mapping in a mid-ventricular short-axis plane during steady-state equilibrium of gadobenate dimeglumine (Gd-BOPTA)(Multihance, Bracco Diagnostics Inc., Princeton, NJ; ~45 min after slow infusion at 0.002 mmol/kg/min). This slow infusion rate was determined empirically based on our extensive experience with large animal (dogs, goats, pigs) CMR experiments. Note that steady-state equilibrium ensures identical concentration of Gd-BOPTA throughout repeated MRI measurements and allows for a fair comparison of post-contrast myocardial and blood T1 measurements by two different pulse sequences. Furthermore, by performing CMR during equilibrium, the specific pulse sequence order was irrelevant.

Experiment 2: Evaluation of Relative Precision in Pigs

Following the completion of separate canine experiments, we conducted an additional experiment to evaluate the precision of AIR compared with MOLLI. Specifically, we imaged 6 female pigs (mean weight = 50 ± 1.4 kg) with normal myocardium to assess scan-to-scan repeatability of MOLLI and AIR. Similar to the canine experiment, in each pig, we performed native cardiac T1 mapping and post-contrast cardiac T1 mapping in a mid-ventricular short-axis plane during steady-state equilibrium of Gd-BOPTA. MOLLI and AIR T1 mapping acquisitions were repeated to quantify scan-to-scan repeatability.

Image Analysis

MOLLI T1 maps were generated in-line on the MRI scanner (Siemens WIP # 448). AIR T1 maps were generated off-line as described in reference (15). Customized software in MATLAB (R2009a, MathWorks, Inc., Natick, MA) was used to manually segment the myocardial contours and blood pools in the left ventricle for each data set separately. Care was taken to avoid partial volume averaging for each contour tracing. T1 was calculated for AIR (15) and MOLLI (10) according to their corresponding equation. Myocardial and blood T1 values were averaged within their respective region of interest. Myocardial ECV was calculated as (35): ECV = (1−hematocrit) × ($R1_m/R1_b$) × 100%, where $R1_m$ is $T1^{-1}$ of myocardium, and $R1_b$ is $T1^{-1}$ of blood, and is the difference between post-contrast and native.

To assess the impact of data quality on analysis, we assessed intra- and inter-observer variability in calculation of T1 and ECV (canine data only). For assessment of intra-observer variability, one observer (K.H) repeated the image analysis, with at least two weeks of separation from the first analysis. For assessment of inter-observer variability, the second observer (D.K) independently analyzed the data. The two observers were blinded to each other, pulse sequence type, and animal identity.

Statistical Analysis

For canine data, we performed a pair-wise t-test to compare T1 and ECV between MOLLI and AIR. We also performed linear regression, concordance correlation (which accounts for

NIH-PA Author Manuscript

NIH-PA Author Manuscript

NIH-PA Author Manuscript

the intercept or additive bias), and Bland-Altman analyses on cardiac T1 and ECV measurements to assess correlation and agreement between MOLLI and AIR data. For assessment of intra- and inter-observer variability, the Bland-Altman analysis was performed on T1 and ECV measurements. A p-value < 0.05 was considered statistically significant.

For pig data, we performed Bland-Altman analysis on myocardial T1 and ECV to calculate the coefficient of repeatability (CR), which is defined as 1.95 × standard deviation of the difference. To avoid confusion with terminology, we note that CR increases with variability in repeated measurements (i.e., higher agreement). All statistical analyses were performed using the Analyse-it software (Analyse-it Software, Ltd., Leeds, United Kingdom).

Results

Experiment 1: Evaluation of Relative Accuracy in Canines

Figure 2 shows representative native and post-contrast MOLLI and AIR cardiac T1 maps of one dog, illustrating typical image quality with both acquisitions. As expected, MOLLI T1 maps derived from 11 images exhibited better overall signal-to-noise ratio (SNR) than AIR T1 maps derived from only 2 images. In this dog (heart rate = 95 bpm), MOLLI and AIR cardiac T1 mapping pulse sequences yielded different T1 and ECV values (see Figure 2 caption for more details).

In 16 dogs (mean heart rate = 98.8 ± 17.5 bpm; mean hematocrit = 0.42 ± 0.02), as expected, mean T1 was significantly different ($p < 0.001$) between MOLLI (891 ± 373 ms) and AIR (1071 ± 503 ms), but, surprisingly, mean ECV between MOLLI (21.8 ± 2.1 %) and AIR (19.6 ± 2.4%) was also significantly different ($p < 0.001$). Pair-wise t-test revealed significant differences for all pairs ($p < 0.0001$), except for post-contrast blood T1 ($p = 0.55$; Table 1). Figure 3 shows scatter plots representing the linear regression and Bland-Altman analyses on T1 and ECV between MOLLI and AIR acquisitions. According to the linear regression and concordance correlation analyses, T1 values were strongly correlated (Pearson's correlation coefficient = 0.99, slope = 1.33, bias = −117.6 ms, $p < 0.0001$; concordance correlation coefficient = 0.87). According to the Bland-Altman analysis, the mean difference in T1 was 179 ms (± 95% confidential interval (CI) = 468/−109 ms), which corresponds to 18% of the mean T1 value (981 ms). According to the linear regression analysis, ECV values were moderately correlated (Pearson's correlation coefficient = 0.65, slope = 0.77, bias = 2.8%, $p < 0.001$). According to the concordance correlation analysis, ECV values were weakly correlated (correlation coefficient = 0.43). According to the Bland-Altman analysis, the mean difference in ECV was −2.2% (± 95% CI = 1.5/−5.9%), which corresponds to 10.8% of the mean ECV value (20.7%).

Experiment 2: Evaluation of Relative Precision in Pigs

Consistent with canine data, in 6 pigs (mean heart rate = 78.1 ± 12.1 bpm; mean hematocrit = 0.30 ± 0.04), mean T1 was significantly different ($p < 0.01$) between MOLLI (899.0 ± 462.8 ms) and AIR (1051.2 ± 635.0 ms), and mean ECV was significantly different also ($p < 0.05$) between MOLLI (25.6 ± 3.1%) and AIR (20.7 ± 1.6%). CR of T1 was considerably

NIH-PA Author Manuscript

NIH-PA Author Manuscript

NIH-PA Author Manuscript

lower for MOLLI (32.5 ms) than AIR (82.3 ms), and CR of ECV was also lower for MOLLI (1.8%) than AIR (4.5%). Recall that, according to the Bland-Altman analysis, lower CR means lower variability (i.e., higher agreement).

Evaluation of Intra- and Inter-Observer Variability in Analysis

For T1 calculations (Figure 4), the intra-observer agreements for MOLLI and AIR data sets were 0.6 ms (upper/lower 95% limits of agreement = 5.3/−4.0 ms) and 0.4 ms (upper/lower 95% limits of agreement = 9.2/−8.5 ms), respectively. These correspond to CR of 4.7 and 8.8 ms for MOLLI and AIR, respectively. The corresponding inter-observer agreements for T1 derived from MOLLI and AIR data sets were 0.009 ms (upper/lower 95% limits of agreement = 9.8/−9.8 ms) and 0.4 ms (upper/lower 95% limits of agreement = 22.7/−21.9 ms), respectively. These correspond to CR of 9.8 and 22.3 ms for MOLLI and AIR, respectively.

For ECV calculations (Figure 5), the intra-observer agreements for MOLLI and AIR data sets were −0.09% (upper/lower 95% limits of agreement = 0.5/−0.7%) and 0.02% (upper/lower 95% limits of agreement = 0.5/−0.4%), respectively. These correspond to CR of 0.6 and 0.5% for MOLLI and AIR, respectively. The corresponding inter-observer agreements for ECV derived from MOLLI and AIR data sets were −0.2% (upper/lower 95% limits of agreement = 1.1/−1.6%) and −0.1% (upper/lower 95% limits of agreement = 1.4/−1.6%), respectively. These correspond to CR of 1.3 and 1.5% for MOLLI and AIR, respectively.

Discussion

In this study, we evaluated, in well-controlled canine and pig experiments, the relative accuracy and precision, as well as intra- and inter-observer variability in data analysis, of T1 and ECV measured with AIR as compared with MOLLI. Canine experiments showed that MOLLI and AIR yield significantly different T1 and ECV values ($p < 0.001$), which have important implications (see below). Both intra- and inter-observer agreements in T1 calculations were higher for MOLLI than AIR, owing to the fact that MOLLI acquires 9 more images than AIR. Interestingly, both intra- and inter-observer agreements in ECV calculations were similar between MOLLI and AIR, possibly owing to off-setting errors when calculating ECV from multiple measurements (native and post-contrast myocardial and blood T1s). Pig experiments showed that MOLLI yields higher precision than AIR, which was expected since AIR acquires 9 less images than MOLLI.

Our observation has important implications for the CMR community. Currently, there are several different variants of inversion-recovery (10,11) and saturation-recovery (12–14,16) based cardiac T1 mapping pulse sequences, as well as a hybrid inversion- and saturation-recovery cardiac T1 mapping pulse sequence (17) and the “TI” scout sequence (18), which is commonly used in conjunction with late gadolinium enhanced MRI (36,37). These different pulse sequences may yield not only different T1 measurements but also ECV measurements, as reported in this study. This implies that CMR researchers must consider the specific pulse sequence when translating published ECV cutoff values into their own studies. It also implies that the CMR community must work towards standardizing cardiac T1 and ECV mapping protocols, in order to move the field forward and increase

NIH-PA Author Manuscript

NIH-PA Author Manuscript

NIH-PA Author Manuscript

reproducibility. The 2013 Society for Cardiovascular Magnetic Resonance and CMR Working Group of the European Society of Cardiology consensus statement (38) is one important step in the right direction towards protocol standardization.

This study has several limitations worth noting. First, we did not test different variants of MOLLI (34,39), because our group has the most experience with the original version of MOLLI (i.e., 3-3-5) that was provided by Siemens. Another study is warranted to test the performance of different variants of MOLLI. Second, we did not compare other inversion-recovery and saturation-recovery based cardiac T1 mapping pulse sequences (11–14,17,18,40). Therefore, our observations may not be directly applicable for other pulse sequences not evaluated in this study. Our study adds to the growing list of studies which compare the performances of different cardiac T1 mapping pulse sequences (11,15,19,41,42). Third, the canines included in this study had a mean heart rate of 98.8 bpm, and pigs had a mean heart rate of 78.1 bpm. This implies that our observation may not be directly applicable for different heart rates and rhythm conditions. Fourth, the animals in this study did not have a prior history of heart disease (assumed to have normal myocardium and supported by ECV measurements). Therefore, our observations may not be directly applicable for hearts with focal and/or diffuse cardiac fibrosis, which changes post-contrast myocardial T1 and ECV values. Fifth, this study did not compare the accuracy of ECV measurements by MOLLI and AIR to histologic quantification of collagen volume fraction. A future study including comprehensive histologic evaluation is warranted to compare the accuracy of ECV measurements between MOLLI and AIR.

In conclusion, this study shows that MOLLI and AIR yield significantly different T1 and ECV values in large animals and that MOLLI yields higher precision than AIR. Both intra- and inter-observer agreements in calculation of T1 were higher for MOLLI than AIR, but intra- and inter-observer agreements in calculation of ECV were similar between MOLLI and AIR. Findings from this study suggest that CMR researchers must consider the specific pulse sequence when translating published ECV cutoff values into their own studies.

Acknowledgments

The authors are grateful for funding support from the NIH (HL116895-01A1), American Heart Association (14GRNT18350028), Ben B. and Iris M. Margolis Foundation, and Wood Family Scholarship Award. The authors would like thank Dr. Vivian Lee for access to her pig MRI studies, and Drs. Nassir Marrouche and Ravi Ranjan for access to their canine MRI studies.

List of Abbreviations

LV	left ventricle
ECV	extracellular volume
CMR	cardiovascular magnetic resonance
b-SSFP	balanced steady state of free precession
AF	atrial fibrillation
R	acceleration rate

NIH-PA Author Manuscript

NIH-PA Author Manuscript

NIH-PA Author Manuscript

bpm	beats per minute
GRAPPA	generalized autocalibrating partially parallel acquisitions
T1	longitudinal relaxation time
LGE	late gadolinium enhanced
TE	echo time
TR	repetition time
AIR	arrhythmia-insensitive-rapid
Gd-BOPTA	gadobenate dimeglumine
TD	saturation-recovery time delay
MOLLI	Modified Look-Locker Inversion-recovery
CR	coefficient of repeatability
SNR	signal-to-noise ratio

References

1. Iles L, Pfluger H, Phrommintikul A, Cherayath J, Aksit P, Gupta SN, Kaye DM, Taylor AJ. Evaluation of diffuse myocardial fibrosis in heart failure with cardiac magnetic resonance contrast-enhanced T1 mapping. J Am Coll Cardiol. 2008; 52(19):1574–1580. [PubMed: 19007595]
2. Sibley CT, Noureldin RA, Gai N, Nacif MS, Liu S, Turkbey EB, Mudd JO, van der Geest RJ, Lima JA, Halushka MK, Bluemke DA. T1 Mapping in Cardiomyopathy at Cardiac MR: Comparison with Endomyocardial Biopsy. Radiology. 2012; 265(3):724–732. [PubMed: 23091172]
3. Messroghli DR, Nordmeyer S, Dietrich T, Dirsch O, Kaschina E, Savvatis K, D Oh-I, Klein C, Berger F, Kuehne T. Assessment of diffuse myocardial fibrosis in rats using small-animal Look-Locker inversion recovery T1 mapping. Circ Cardiovasc Imaging. 2011; 4(6):636–640. [PubMed: 21917782]
4. Miller CA, Naish JH, Bishop P, Coutts G, Clark D, Zhao S, Ray SG, Yonan N, Williams SG, Flett AS, Moon JC, Greiser A, Parker GJ, Schmitt M. Comprehensive validation of cardiovascular magnetic resonance techniques for the assessment of myocardial extracellular volume. Circ Cardiovasc Imaging. 2013; 6(3):373–383. [PubMed: 23553570]
5. Flett AS, Hayward MP, Ashworth MT, Hansen MS, Taylor AM, Elliott PM, McGregor C, Moon JC. Equilibrium contrast cardiovascular magnetic resonance for the measurement of diffuse myocardial fibrosis: preliminary validation in humans. Circulation. 2010; 122(2):138–144. [PubMed: 20585010]
6. Kehr E, Sono M, Chugh SS, Jerosch-Herold M. Gadolinium-enhanced magnetic resonance imaging for detection and quantification of fibrosis in human myocardium in vitro. Int J Cardiovasc Imaging. 2008; 24(1):61–68. [PubMed: 17429755]
7. Jerosch-Herold M, Sheridan DC, Kushner JD, Nauman D, Burgess D, Dutton D, Alharethi R, Li D, Hershberger RE. Cardiac magnetic resonance imaging of myocardial contrast uptake and blood flow in patients affected with idiopathic or familial dilated cardiomyopathy. Am J Physiol Heart Circ Physiol. 2008; 295(3):H1234–H1242. [PubMed: 18660445]
8. White SK, Sado DM, Fontana M, Banypersad SM, Maestrini V, Flett AS, Piechnik SK, Robson MD, Hausenloy DJ, Sheikh AM, Hawkins PN, Moon JC. T1 Mapping for Myocardial Extracellular Volume Measurement by CMR: Bolus Only Versus Primed Infusion Technique. JACC Cardiovascular imaging. 2013; 6(9):955–962. [PubMed: 23582361]
9. Kramer CM, Chandrashekhar Y, Narula J. T1 mapping by CMR in cardiomyopathy: a noninvasive myocardial biopsy? JACC Cardiovascular imaging. 2013; 6(4):532–534. [PubMed: 23579019]

NIH-PA Author Manuscript NIH-PA Author Manuscript NIH-PA Author Manuscript

10. Messroghli DR, Radjenovic A, Kozerke S, Higgins DM, Sivananthan MU, Ridgway JP. Modified Look-Locker inversion recovery (MOLLI) for high-resolution T1 mapping of the heart. Magnetic resonance in medicine : official journal of the Society of Magnetic Resonance in Medicine / Society of Magnetic Resonance in Medicine. 2004; 52(1):141–146.
11. Piechnik SK, Ferreira VM, Dall'Armellina E, Cochlin LE, Greiser A, Neubauer S, Robson MD. Shortened Modified Look-Locker Inversion recovery (ShMOLLI) for clinical myocardial T1-mapping at 1.5 and 3 T within a 9 heartbeat breathhold. Journal of cardiovascular magnetic resonance : official journal of the Society for Cardiovascular Magnetic Resonance. 2010; 12:69. [PubMed: 21092095]
12. Song T, Stainsby JA, Ho VB, Hood MN, Slavin GS. Flexible cardiac T1 mapping using a modified Look-Locker acquisition with saturation recovery. Magnetic resonance in medicine : official journal of the Society of Magnetic Resonance in Medicine/Society of Magnetic Resonance in Medicine. 2012; 67(3):622–627.
13. Slavin, GSHM.; Ho, VB.; Stainsby, JA. Breath-Held Myocardial T1 Mapping Using Multiple Single-Point Saturation Recovery. Proceedings of the 20th Annual Meeting of ISMRM; Melbourne, Australia. 2012. p. 1244
14. Slavin, G.; Stainsby, J. True T1 mapping with SMART1Map (saturation method using adaptive recovery times for cardiac T1 mapping): a comparison with MOLLI. Proceedings of the 16th Annual Meeting of SCMR Scientific Sessions; San Francisco, CA, USA. 2013. p. P3
15. Fitts M, Breton E, Kholmovski EG, Dosdall DJ, Vijayakumar S, Hong KP, Ranjan R, Marrouche NF, Axel L, Kim D. Arrhythmia insensitive rapid cardiac T1 mapping pulse sequence. Magnetic resonance in medicine : official journal of the Society of Magnetic Resonance in Medicine / Society of Magnetic Resonance in Medicine. 2013; 70(5):1274–1282.
16. Chow K, Flewitt JA, Green JD, Pagano JJ, Friedrich MG, Thompson RB. Saturation recovery single-shot acquisition (SASHA) for myocardial T mapping. Magnetic resonance in medicine : official journal of the Society of Magnetic Resonance in Medicine / Society of Magnetic Resonance in Medicine. 2013
17. Weingartner S, Akcakaya M, Basha T, Kissinger KV, Goddu B, Berg S, Manning WJ, Nezafat R. Combined saturation/inversion recovery sequences for improved evaluation of scar and diffuse fibrosis in patients with arrhythmia or heart rate variability. Magnetic resonance in medicine : official journal of the Society of Magnetic Resonance in Medicine / Society of Magnetic Resonance in Medicine. 2013
18. Gupta A, Lee VS, Chung YC, Babb JS, Simonetti OP. Myocardial infarction: optimization of inversion times at delayed contrast-enhanced MR imaging. Radiology. 2004; 233(3):921–926. [PubMed: 15516607]
19. Robson MD, Piechnik SK, Tunnicliffe EM, Neubauer S. T1 measurements in the human myocardium: The effects of magnetization transfer on the SASHA and MOLLI sequences. Magnetic resonance in medicine : official journal of the Society of Magnetic Resonance in Medicine / Society of Magnetic Resonance in Medicine. 2013
20. Gai N, Stehning C, Nacif M, Bluemke D. Modified Look-Locker T1 evaluation using Bloch simulations: Human and phantom validation. Magnetic Resonance in Medicine. 2012
21. Chow, K.; Flewitt, JA.; Pagano, JJ.; Green, JD.; Friedrich, MG.; Thompson, RB. MOLLI T_1 Values Have Systematic T_2 and Inversion Efficiency Dependent Errors. Proceedings of the 20th Annual Meeting of ISMRM; Melbourne, Australia. 2012. p. 395
22. Kellman P, Herzka DA, Hansen MS. Adiabatic inversion pulses for myocardial T1 mapping. Magnetic resonance in medicine : official journal of the Society of Magnetic Resonance in Medicine / Society of Magnetic Resonance in Medicine. 2014; 71(4):1428–1434.
23. Kampf T, Helluy X, Gutjahr FT, Winter P, Meyer CB, Jakob PM, Bauer WR, Ziener CH. Myocardial perfusion quantification using the T1 -based FAIR-ASL method: the influence of heart anatomy, cardiopulmonary blood flow and look-locker readout. Magnetic resonance in medicine : official journal of the Society of Magnetic Resonance in Medicine / Society of Magnetic Resonance in Medicine. 2014; 71(5):1784–1797.
24. Kim D, Oesingmann N, McGorty K. Hybrid adiabatic-rectangular pulse train for effective saturation of magnetization within the whole heart at 3 T. Magnetic resonance in medicine :

NIH-PA Author Manuscript

NIH-PA Author Manuscript

NIH-PA Author Manuscript

official journal of the Society of Magnetic Resonance in Medicine / Society of Magnetic Resonance in Medicine. 2009; 62(6):1368–1378.

25. Hong K, Kholmovski EG, McGann CJ, Ranjan R, Kim D. Comparison of ECV measurements during equilibrium between IR- and SR-based cardiac T1 mapping. Journal of Cardiovascular Magnetic Resonance. 2014; 16(Suppl 1):P53.
26. Hong KP, Kholmovski EG, McGann CJ, Ranjan R, Kim D. Comparison of canine ECV measurements derived from CMR: bolus injection vs. slow infusion of Gd-BOPTA. Journal of Cardiovascular Magnetic Resonance. 2014; 16(Suppl 1):P64.
27. Koopmann M, Hong K, Kholmovski EG, Huang EC, Hu N, Ying J, Levenson R, Vijayakumar S, Dosdall DJ, Ranjan R, Kim D. Post-contrast myocardial T1 and ECV disagree in a longitudinal canine study. NMR in Biomedicine. 2014; 27(8):988–995. [PubMed: 24865566]
28. Kellman P, Wilson JR, Xue H, Bandettini WP, Shanbhag SM, Druey KM, Ugander M, Arai AE. Extracellular volume fraction mapping in the myocardium, part 2: initial clinical experience. Journal of cardiovascular magnetic resonance : official journal of the Society for Cardiovascular Magnetic Resonance. 2012; 14:64. [PubMed: 22967246]
29. Ugander M, Oki AJ, Hsu LY, Kellman P, Greiser A, Aletras AH, Sibley CT, Chen MY, Bandettini WP, Arai AE. Extracellular volume imaging by magnetic resonance imaging provides insights into overt and sub-clinical myocardial pathology. Eur Heart J. 2012; 33(10):1268–1278. [PubMed: 22279111]
30. Brouwer WP, Baars EN, Germans T, de Boer K, Beek AM, van der Velden J, van Rossum AC, Hofman MB. In-vivo T1 cardiovascular magnetic resonance study of diffuse myocardial fibrosis in hypertrophic cardiomyopathy. Journal of cardiovascular magnetic resonance : official journal of the Society for Cardiovascular Magnetic Resonance. 2014; 16(1):28. [PubMed: 24766828]
31. Kellman P, Hansen MS. T1-mapping in the heart: accuracy and precision. Journal of cardiovascular magnetic resonance : official journal of the Society for Cardiovascular Magnetic Resonance. 2014; 16(1):2. [PubMed: 24387626]
32. Griswold MA, Jakob PM, Heidemann RM, Nittka M, Jellus V, Wang J, Kiefer B, Haase A. Generalized autocalibrating partially parallel acquisitions (GRAPPA). Magnetic resonance in medicine : official journal of the Society of Magnetic Resonance in Medicine / Society of Magnetic Resonance in Medicine. 2002; 47(6):1202–1210.
33. Bieri O, Markl M, Scheffler K. Analysis and compensation of eddy currents in balanced SSFP. Magnetic resonance in medicine : official journal of the Society of Magnetic Resonance in Medicine / Society of Magnetic Resonance in Medicine. 2005; 54(1):129–137.
34. Messroghli DR, Greiser A, Frohlich M, Dietz R, Schulz-Menger J. Optimization and validation of a fully-integrated pulse sequence for modified look-locker inversion-recovery (MOLLI) T1 mapping of the heart. Journal of magnetic resonance imaging : JMRI. 2007; 26(4):1081–1086. [PubMed: 17896383]
35. Arheden H, Saeed M, Higgins CB, Gao DW, Bremerich J, Wyttenbach R, Dae MW, Wendland MF. Measurement of the distribution volume of gadopentetate dimeglumine at echo-planar MR imaging to quantify myocardial infarction: comparison with 99mTc-DTPA autoradiography in rats. Radiology. 1999; 211(3):698–708. [PubMed: 10352594]
36. Kim RJ, Fieno DS, Parrish TB, Harris K, Chen EL, Simonetti O, Bundy J, Finn JP, Klocke FJ, Judd RM. Relationship of MRI delayed contrast enhancement to irreversible injury, infarct age, and contractile function. Circulation. 1999; 100(19):1992–2002. [PubMed: 10556226]
37. Kim RJ, Wu E, Rafael A, Chen EL, Parker MA, Simonetti O, Klocke FJ, Bonow RO, Judd RM. The use of contrast-enhanced magnetic resonance imaging to identify reversible myocardial dysfunction. N Engl J Med. 2000; 343(20):1445–1453. [PubMed: 11078769]
38. Moon JC, Messroghli DR, Kellman P, Piechnik SK, Robson MD, Ugander M, Gatehouse PD, Arai AE, Friedrich MG, Neubauer S, Schulz-Menger J, Schelbert EB. Myocardial T1 mapping and extracellular volume quantification: a Society for Cardiovascular Magnetic Resonance (SCMR) and CMR Working Group of the European Society of Cardiology consensus statement. Journal of cardiovascular magnetic resonance : official journal of the Society for Cardiovascular Magnetic Resonance. 2013; 15(1):92. [PubMed: 24124732]
39. Kellman P, Wilson JR, Xue H, Ugander M, Arai AE. Extracellular volume fraction mapping in the myocardium, part 1: evaluation of an automated method. Journal of cardiovascular magnetic

NIH-PA Author Manuscript

NIH-PA Author Manuscript

NIH-PA Author Manuscript

resonance : official journal of the Society for Cardiovascular Magnetic Resonance. 2012; 14:63. [PubMed: 22963517]

40. Chow K, Flewitt JA, Green JD, Pagano JJ, Friedrich MG, Thompson RB. Saturation recovery single-shot acquisition (SASHA) for myocardial T1 mapping. Magnetic Resonance in Medicine. 2014; 71(6):2082–2095. [PubMed: 23881866]
41. Nacif MS, Turkbey EB, Gai N, Nazarian S, van der Geest RJ, Noureldin RA, Sibley CT, Ugander M, Liu S, Arai AE, Lima JA, Bluemke DA. Myocardial T1 mapping with MRI: comparison of look-locker and MOLLI sequences. Journal of magnetic resonance imaging : JMRI. 2011; 34(6): 1367–1373. [PubMed: 21954119]
42. Roujol S, Weingartner S, Foppa M, Chow K, Kawaji K, Ngo LH, Kellman P, Manning WJ, Thompson RB, Nezafat R. Accuracy, Precision, and Reproducibility of Four T1 Mapping Sequences: A Head-to-Head Comparison of MOLLI, ShMOLLI, SASHA, and SAPPHIRE. Radiology. 2014:140–296.

NIH-PA Author Manuscript
NIH-PA Author Manuscript
NIH-PA Author Manuscript

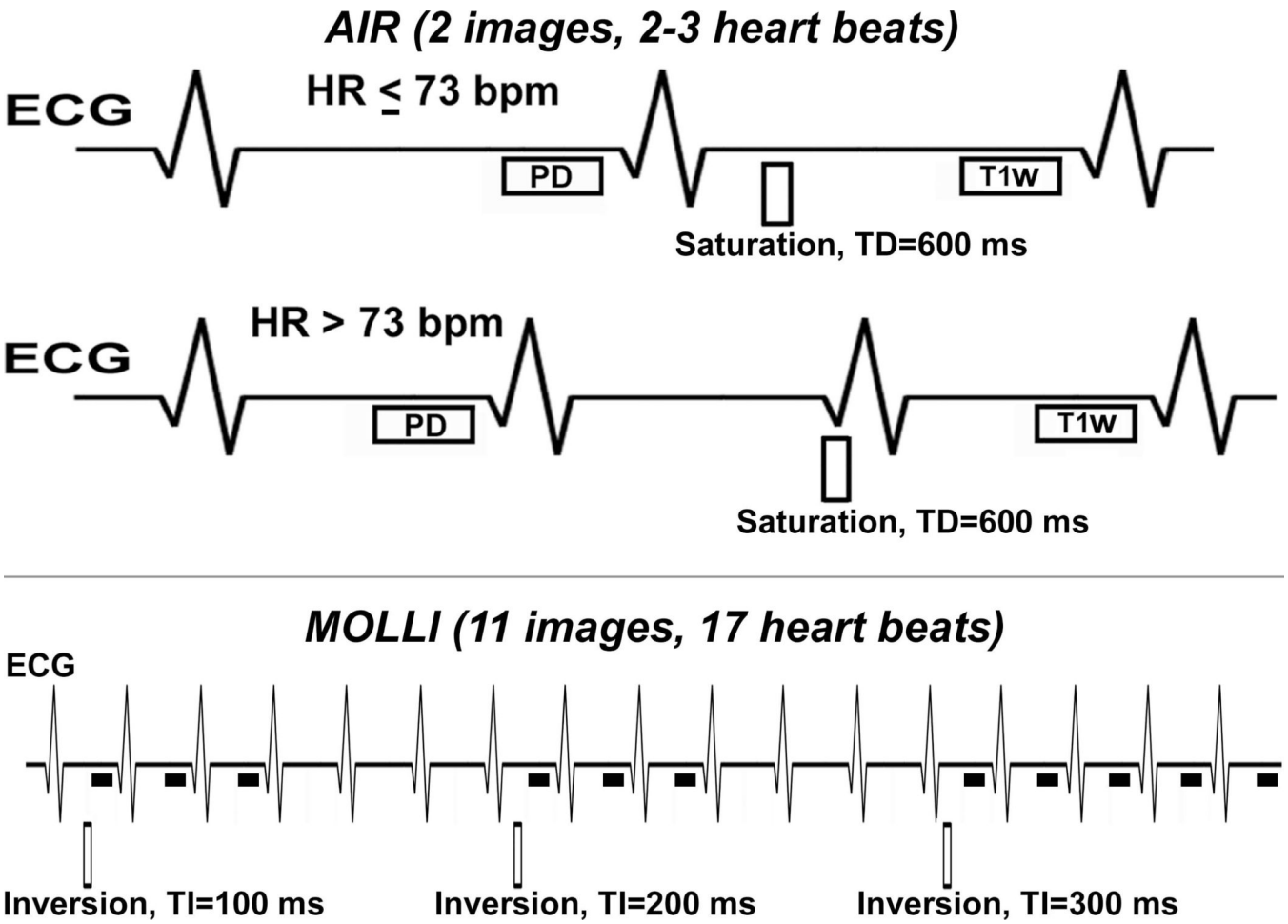

Figure 1.

Schematic of AIR (top row) and (bottom) MOLLI cardiac T1 mapping pulse sequences. AIR acquires one proton density and one T1-weighted image in succession with scan time of 2–3 heart beats, depending on heart rate as shown. MOLLI acquires 11 images with scan time of 17 heart beats, following three inversion pulses as shown (i.e., 3-3-5).

NIH-PA Author Manuscript
NIH-PA Author Manuscript
NIH-PA Author Manuscript

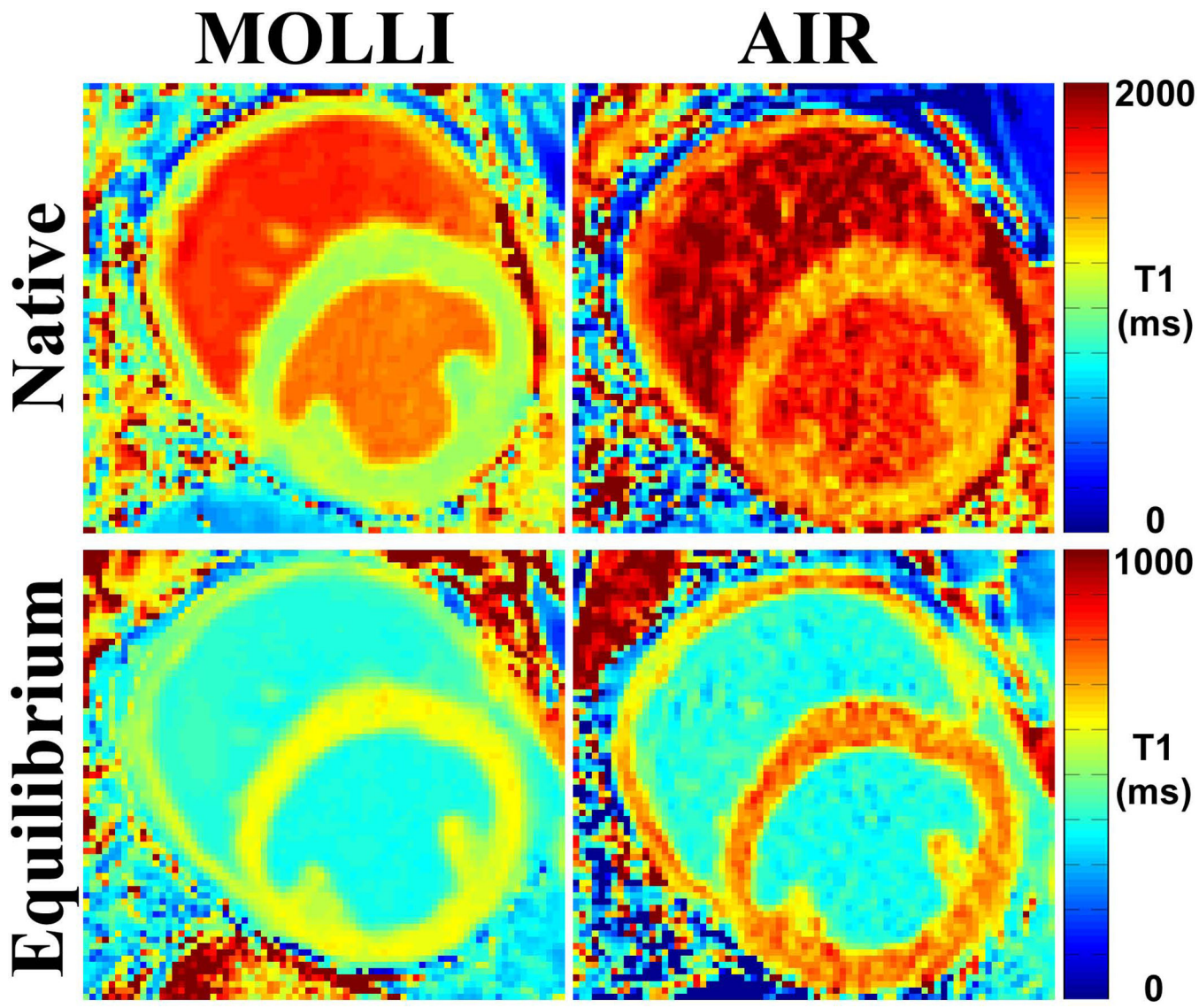

Figure 2.

Representative cardiac T1 maps of one dog (heart rate = 94.5 bpm) acquired with MOLLI (left) and AIR (right) cardiac T1 mapping pulse sequences: native (top row) and post-contrast (bottom row). These examples illustrate typical image quality produced by MOLLI and AIR. Compared with AIR T1 maps derived from only 2 images, MOLLI T1 maps derived from 11 images exhibited higher overall SNR. Native myocardial and blood T1 values were different (native myocardial T1 was 1074.1 ms (MOLLI) and 1373.4 ms (AIR); native blood T1 was 1492.7 ms (MOLLI) and 1692.9 ms (AIR). Post-contrast myocardial T1 was also different (605.5 ms [MOLLI] and 724.5 ms [AIR]), but post-contrast blood T1 was not different (389.2 ms [MOLLI] and 384.8 ms [AIR]). These differences in T1 resulted in discordant ECV measurements (22.0% and 18.8% for MOLLI and AIR, respectively).

NIH-PA Author Manuscript
NIH-PA Author Manuscript
NIH-PA Author Manuscript

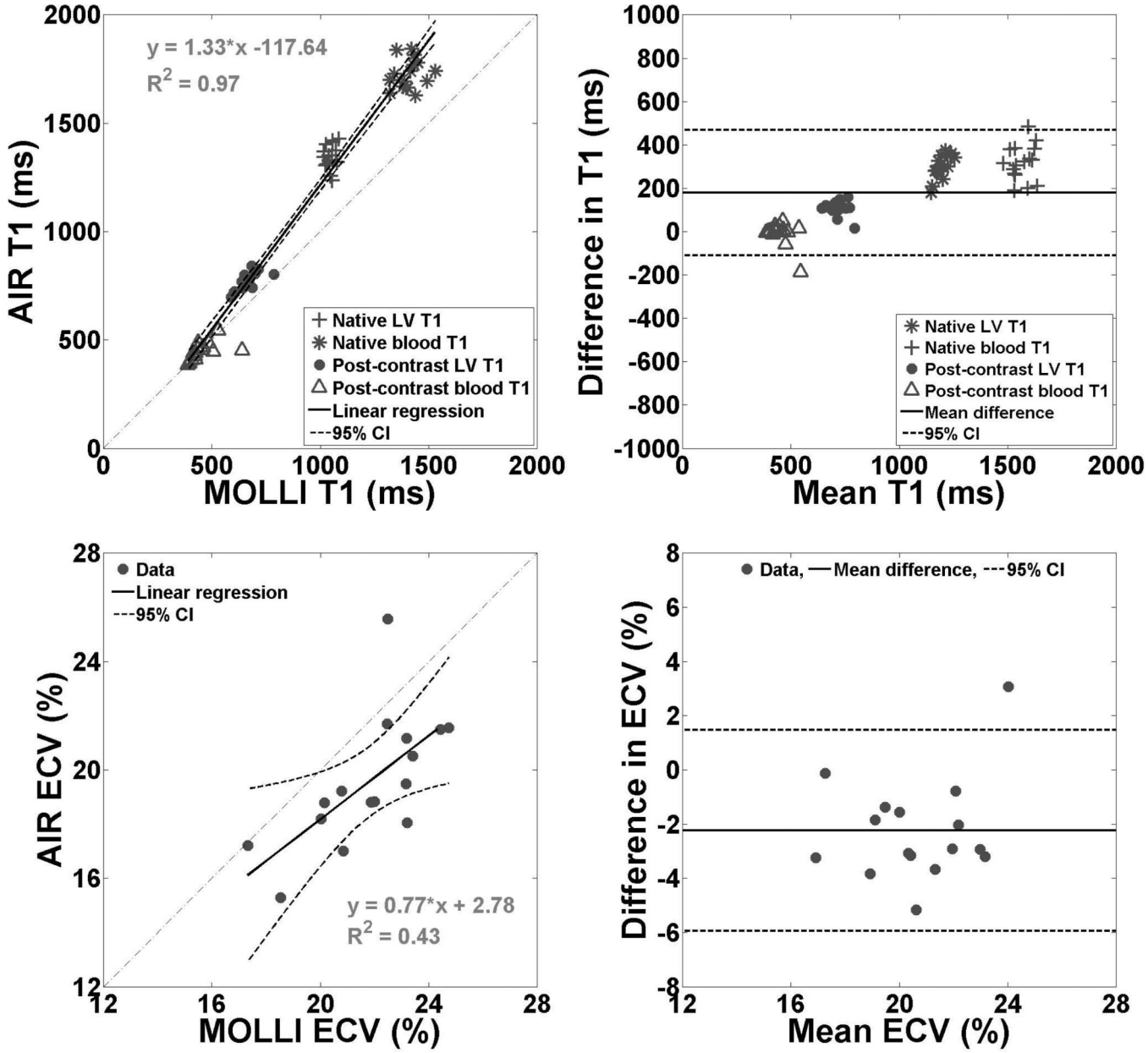

Figure 3.

Scatter plots representing linear regression (left column) and Bland-Altman (right column) analyses: T1 (top row) and ECV (bottom row) derived from MOLLI and AIR cardiac T1 mapping pulse sequences in 16 dogs. According to the linear regression and concordance correlation analyses, T1 values were strongly correlated (Pearson's correlation coefficient = 0.99, slope = 1.33, bias = −117.6 ms, $p < 0.0001$; concordance correlation coefficient = 0.87). According to the Bland-Altman analysis, the mean difference in T1 was 179 ms (± 95% confidential interval (CI) = 468/−109 ms), which corresponds to 18% of the mean T1 value (981 ms). For ease of interpretation, the Bland-Altman plot for T1 was displayed with y-axis ranging from −1000 to 1000 ms (i.e., approximately −100 to 100 % of the mean value of 981 ms). According to the linear regression analysis, ECV values derived were

NIH-PA Author Manuscript

NIH-PA Author Manuscript

NIH-PA Author Manuscript

moderately correlated (Pearson's correlation coefficient = 0.65, slope = 0.77, bias = 2.8%, $p < 0.001$). According to the concordance correlation analysis, ECV values were weakly correlated (correlation coefficient = 0.43). According to the Bland-Altman analysis, the mean difference in ECV was −2.2% (± 95% CI = 1.5/−5.9%), which corresponds to 10.8% of the mean ECV value (20.7%). For ease of interpretation, the Bland-Altman plot for ECV was displayed with y-axis ranging from −8 to 8% (i.e., approximately −10 to 10 % of the mean value of 20.7%). Difference defined as AIR - MOLLI.

NIH-PA Author Manuscript
NIH-PA Author Manuscript
NIH-PA Author Manuscript

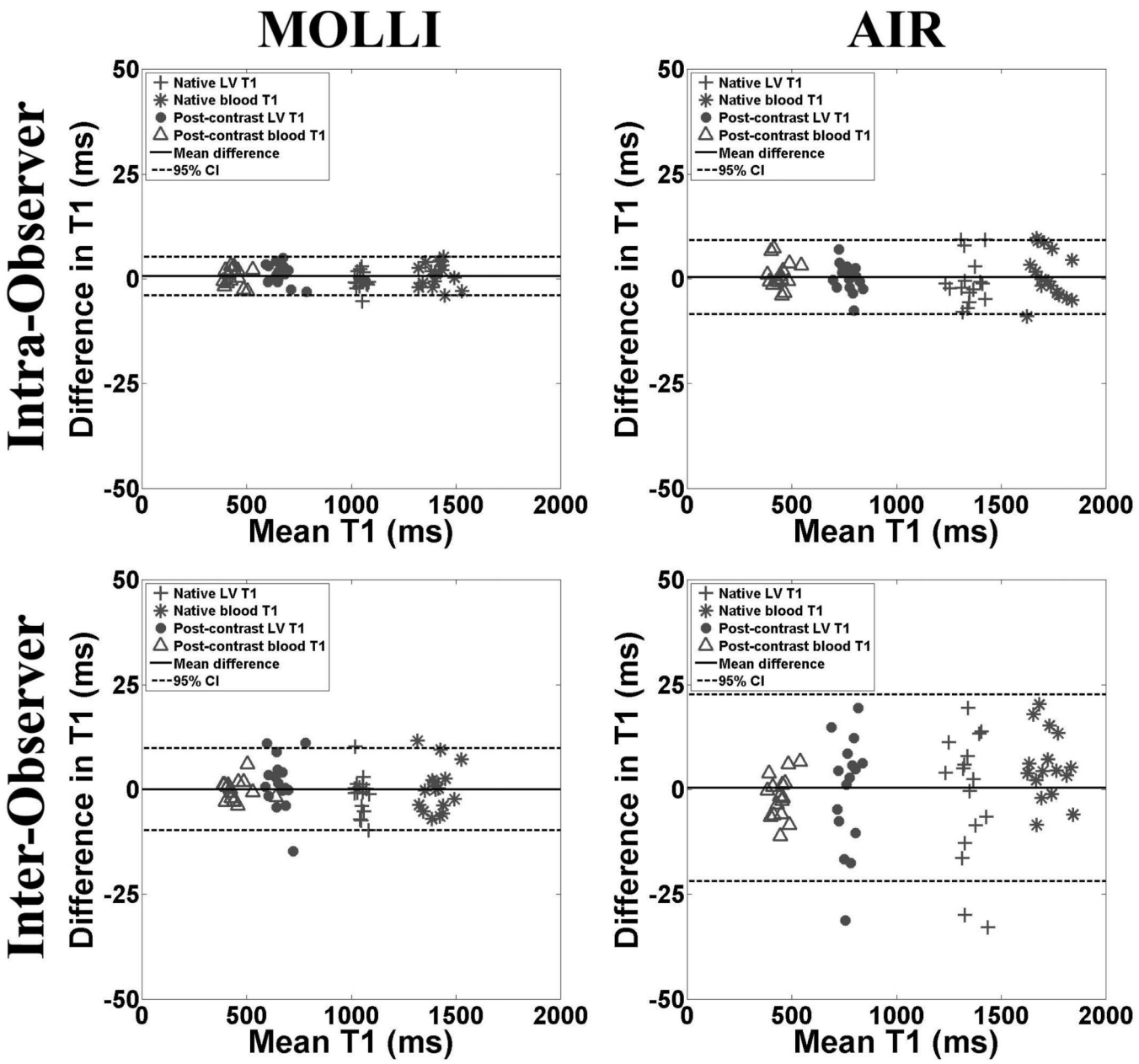

Figure 4.

Scatter plots representing the intra- (top row) and inter-observer (bottom row) agreements in calculation of T1 derived from MOLLI (left column) and AIR (right column) data sets. For intra-observer agreement, the mean difference in T1 was 0.6 ms (upper/lower 95% limits of agreement = 5.3/−4.0 ms) and 0.4 ms (upper/lower 95% limits of agreement = 9.2/−8.5 ms) for MOLLI and AIR, respectively. For inter-observer agreement, the mean difference in T1 was 0.009 ms (upper/lower 95% limits of agreement = 9.8/−9.8 ms) and 0.4 ms (upper/lower 95% limits of agreement = 22.7/−21.9 ms) for MOLLI and AIR, respectively. Note that CR was lower MOLLI than AIR, suggesting higher overall SNR for MOLLI than AIR. For ease of interpretation, the Bland-Altman plots were displayed with y-axis ranging from −50 to 50

ms (i.e., approximately −5 to 5 % of the mean value of 1000 ms). Solid and dotted lines represent the mean difference and 95% confidence intervals, respectively.

NIH-PA Author Manuscript
NIH-PA Author Manuscript
NIH-PA Author Manuscript

NIH-PA Author Manuscript

NIH-PA Author Manuscript

NIH-PA Author Manuscript

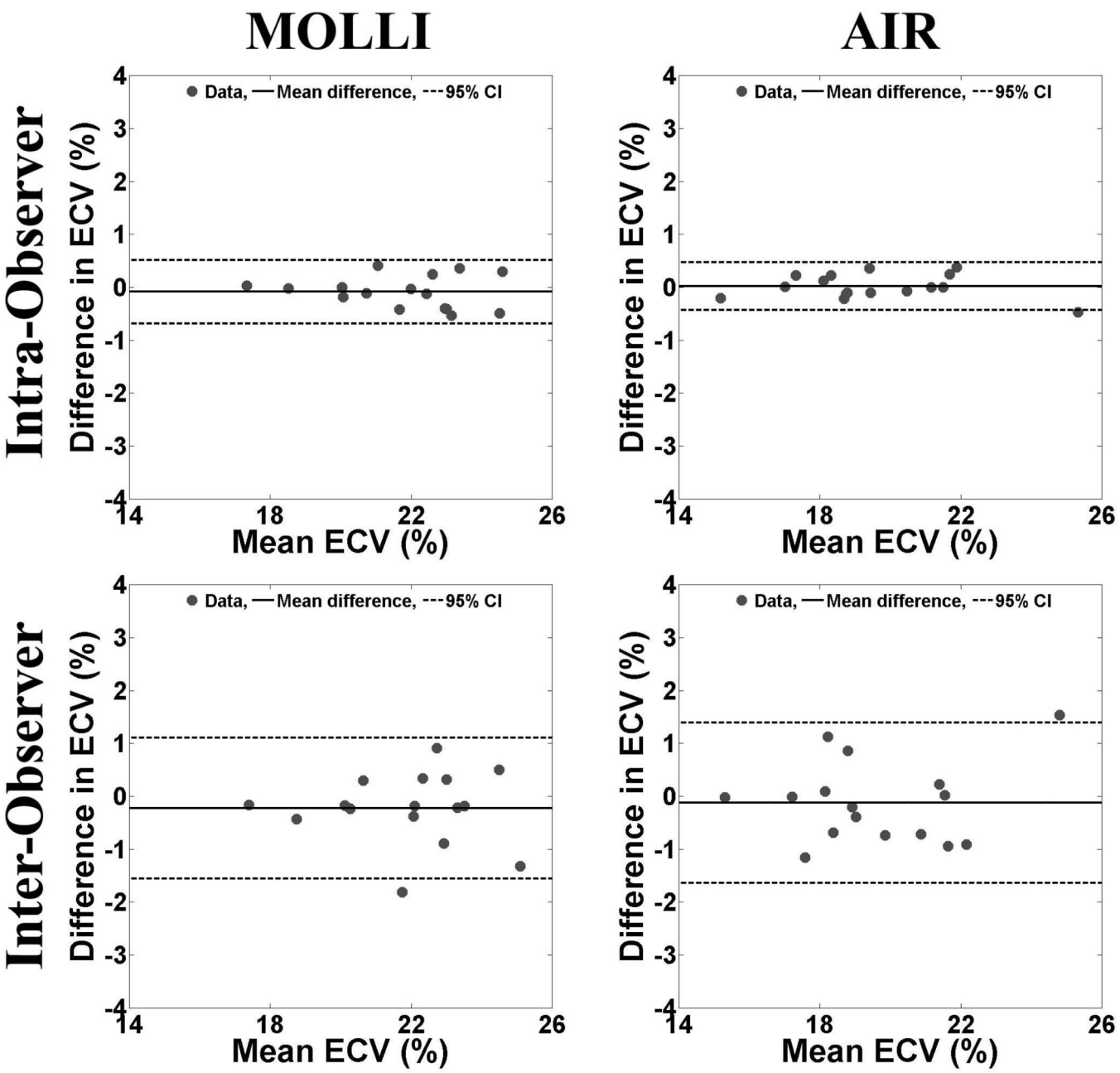

Figure 5.

Scatter plots representing the intra- (top row) and inter-observer (bottom row) agreements in calculation of ECV derived from MOLLI (left column) and AIR (right column) data sets. For intra-observer agreement, the mean difference in ECV was −0.09% (upper/lower 95% limits of agreement = 0.5/−0.7%) and 0.02% (upper/lower 95% limits of agreement = 0.5/−0.4%) for MOLLI and AIR, respectively. For inter-observer agreement, the mean difference in ECV was −0.2% (upper/lower 95% limits of agreement = 1.1/−1.6%) and −0.1% (upper/lower 95% limits of agreement = 1.4/−1.6%) for MOLLI and AIR, respectively. Note that CR was similar between MOLLI and AIR, possibly due to off-setting errors from multiple measurements. For ease of interpretation, the Bland-Altman plots were

displayed with y-axis ranging from −4 to 4% (i.e., approximately −5 to 5 % of the mean value of 20%). Solid and dotted lines represent the mean difference and 95% confidence intervals, respectively.

NIH-PA Author Manuscript
NIH-PA Author Manuscript
NIH-PA Author Manuscript

NIH-PA Author Manuscript

NIH-PA Author Manuscript

NIH-PA Author Manuscript

Table 1

Pair-wise t-test statistics comparing the different subgroups of T1 derived from MOLLI and AIR cardiac T1 mapping pulse sequences: native myocardial T1, native blood T1, post-contrast myocardial T1, and post-contrast blood T1. T1 value represents mean ± standard deviation.

Tissue Type	MOLLI	AIR	*p*
Native myocardial T1	1047.0 ± 21.3 ms	1345.2 ± 55.1 ms	< 0.0001
Native blood T1	1407.7 ± 57.5 ms	1724.7 ± 68.5 ms	< 0.0001
Post-contrast myocardial T1	659.0 ± 50.1 ms	768.0 ± 42.0 ms	< 0.0001
Post-contrast blood T1	452.1 ± 64.1 ms	444.0 ± 41.1 ms	0.55